Tailoring of amplification spectrum using dc-field for high-precision two-wave mixing adaptive interferometry with CdTe

Konstantin Shcherbin, Marvin B. Klein, Dean R. Evans

Konstantin Shcherbin, Marvin B. Klein, Dean R. Evans, "Tailoring of amplification spectrum using dc-field for high-precision two-wave mixing adaptive interferometry with CdTe," Proc. SPIE 10934, Optical, Opto-Atomic, and Entanglement-Enhanced Precision Metrology, 109341G (1 March 2019); doi: 10.1117/12.2514802

Event: SPIE OPTO, 2019, San Francisco, California, United States

Tailoring of amplification spectrum using dc-field for high-precision two-wave mixing adaptive interferometry with CdTe

Konstantin Shcherbin*[a], Marvin B. Klein[b], Dean R. Evans[c]
[a]Institute of Physics, National Academy of Sciences, Prospekt Nauki 46, 03680 Kiev, Ukraine; [b]Intelligent Optical Systems, Inc., 2520 West 237th Street, Torrance, CA 90505, USA; [c]Air Force Research Laboratory, Materials and Manufacturing Directorate, Wright-Patterson Air Force Base, OH 45433, USA

ABSTRACT

Two-wave mixing adaptive interferometers based on photorefractive crystals allow for precise remote detection of small displacements. Using dynamic holograms, they compensate for ambient disturbances in factory environments and can process speckled beams with complicated wavefronts. Linear phase-to-intensity conversion with maximum sensitivity is achieved when the response becomes local when a dc-field is applied to the photorefractive crystal. In the present work we study experimentally the change of the shape of the amplification spectrum induced by a dc field in the two-wave mixing geometry. The shape of the spectrum is used for identification of the type of response (local or nonlocal). High sensitivity for detection of surface displacements is demonstrated for a two-wave mixing interferometer with a dc-biased CdTe:Ge crystal.

Keywords: Laser ultrasonics, dynamic holography, photorefractive effect, two-wave mixing, adaptive interferometer, photorefractive semiconductor, cadmium telluride

1. INTRODUCTION

Laser ultrasonics is a totally remote technique for nondestructive testing, flaw detection, and thickness measurements. It provides the sensitivity of the conventional ultrasonic technique with the flexibility of optical systems. A pulsed laser is used for ultrasonics generation, as is shown in Fig. 1a. An ultrasonic wave is excited in the sample under inspection, when a pulse from a high peak power pulsed laser is absorbed at the surface. A laser ultrasonic receiver is used for detection of ultrasonic echoes at the surface of the material by interferometry. A probe, usually continuous-wave, beam is sent to the surface. The reflected light wave becomes phase modulated because of the displacement of the surface. The phase modulation is converted into intensity modulation by the interferometer.

Conventional interferometers cannot process speckled beams reflected from rough surfaces. In addition, they require precise path-length stabilization for effective operation in the quadrature condition. Adaptive interferometers based on two-wave mixing (TWM) may overcome these disadvantages. In such interferometers a conventional beam-splitter is replaced by a dynamic hologram recorded usually in a photorefractive crystal (see Fig. 1b). The signal wave scattered from the vibrating surface of an object under inspection and a separate reference wave interfere in the crystal and record a photorefractive grating. The grating serves as a holographic beam-splitter[1-3]. The holographic property enables effective processing of complicated wavefronts of the speckled object beam. As the hologram is dynamic, it adapts to slow wavefront variations of the signal wave with a response time of the grating, ensuring continuous compensation for temporal disturbances in the environment. At the same time, ultrasonic vibrations are much faster than the grating response time. That is why the hologram may be considered as fixed grating for the fast phase variations related to the ultrasound. Thus, conversion of the phase modulation to intensity modulation becomes possible at ultrasonic frequencies. In addition, operation in quadrature conditions may be maintained automatically in many configurations of the nonlinear interaction, for example, when an external electric field is applied to the crystal.

*kshcherb@iop.kiev.ua

Optical, Opto-Atomic, and Entanglement-Enhanced Precision Metrology, edited by Selim M. Shahriar, Jacob Scheuer, Proc. of SPIE Vol. 10934, 109341G · © 2019 SPIE · CCC code: 0277-786X/19/$18 · doi: 10.1117/12.2514802

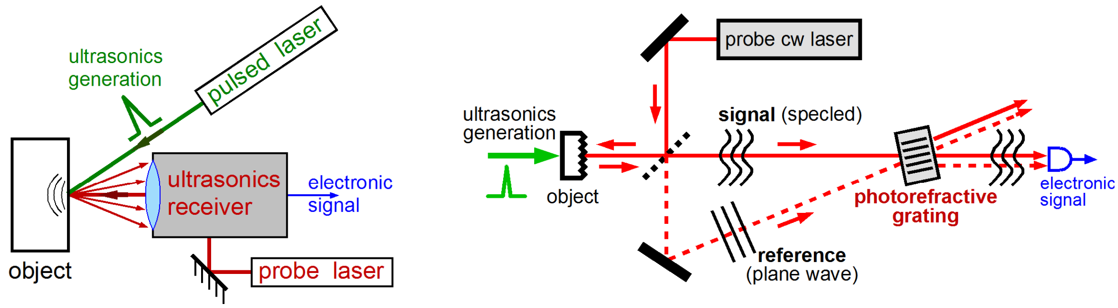

(a) (b)

Figure 1. Schematic representations: (a) – laser ultrasonics technique, (b) – two-wave mixing adaptive interferometer.

In the present work we study a TWM adaptive interferometer using the semi-insulating CdTe:Ge. The type of crystal response (local or nonlocal) is determined from the spectra of the coupling constant in two-beam coupling with non-degenerate frequencies and with zero or a finite external dc field applied to the crystal. The performance of interferometer is compared under different experimental conditions when the nonlocal or local component of the grating dominates.

2. PHASE-TO-INTENSITY CONVERSION IN AN ADAPTIVE INTERFEROMETER

The linear conversion of phase modulation to intensity modulation with maximum sensitivity is achieved in an interferometer when the waves are in quadrature, i.e., when the phase shift between interfering waves is $\pm\pi/2$. Let us consider the case of an adaptive interferometer with a dynamic grating. The signal beam and the reference (pump) beam interfere in the photorefractive crystal as shown in Fig. 1b. This results in the recording of a refractive index grating. The grating recorded by diffusion charge transport is $\pm\pi/2$ shifted with respect to the interference pattern. The pump beam diffracts from the grating with a diffraction efficiency η and its diffracted part interferes with the transmitted part of the signal wave. For low diffraction efficiency $\eta << 1$ the amplitude of the signal wave behind the crystal may be presented

$$A_S = \left(\sqrt{1-\eta}\,A_S^0 \exp\left[i\Phi + i\varphi(t)\right] + \sqrt{\eta}\,A_P^0\right), \tag{1}$$

where A_S^0 and A_P^0 are amplitudes of the interfering waves at the crystal input, Φ is the phase shift between interference fringes and refractive index grating and $\varphi(t)$ models the fast phase modulation induced by the ultrasonic surface displacement, $\varphi(t) = \Delta\varphi \sin(2\pi f t)$ with low amplitude ($\Delta\varphi << \pi/2$) and high frequency ($2\pi f >> 1/\tau_{SC}$, τ_{SC} is response time of the grating). This yields the intensity of the transmitted signal beam

$$I_S(t) = (1-\eta)I_S^0 + \eta I_P^0 + 2\sqrt{\eta(1-\eta)I_S^0 I_P^0}\sin\left(\Phi + \varphi(t)\right) \tag{2}$$

with I_S^0 and I_P^0 being the intensities of the signal and pump beams at the crystal input. Thus, the amplitude of the output intensity modulation is given by

$$\Delta I_S \propto \sin\left(\Phi + \Delta\varphi\right). \tag{3}$$

For the photorefractive grating $\Phi = \pm\pi/2$ and therefore $\sin(\Phi + \Delta\varphi) \approx 1$. The alternative component of intensity, intensity modulation, is negligible for small $\Delta\varphi$, and the sensitivity of the photorefractive grating to the phase modulation detection is very low.

In order to overcome this drawback various innovative techniques have been demonstrated for increasing the sensitivity by imposing quadrature conditions for adaptive interferometers with nonlocal photorefractive holograms. These are the use of anisotropic diffraction[2] including mixing of waves with linear and elliptic polarizations[4], differential light power detection[3], step-like translation of the interference pattern using external phase modulation of one of the recording beams[5], combinations of different techniques, etc.

For a local grating with $\Phi = 0, \pi$ the quadrature conditions are fulfilled automatically. The intensity modulation linearly depends on the phase modulation $\Delta I \propto \Delta\varphi$, as is confirmed by Eq. (3). Thus, the local response is of particular interest for adaptive interferometers. That is why the capability of local gratings in liquid crystal light valves[6] and in gain media[7] have been studied. Also, the operation of digital holography with electronic processing and control of the phase shift between interference pattern and index grating has been demonstrated[8].

On the other hand, the grating shift can be modified in photorefractive crystal by application of a dc field[9]. The grating becomes local when drift transport of the photoexcited charge carriers dominates diffusion, while the drift length is much smaller than the grating period[9] Λ. In addition, an external field results in an enhancement of the photorefractive effect. That is why the dc-field technique is very promising for applications[10].

3. TWO-WAVE MIXING GAIN SPECTRA FOR NONLOCAL AND LOCAL RESPONSE

The coupling constant, which is generally complex, $\gamma = \gamma' + i\gamma''$, describes TWM using a dynamic hologram. It connects the amplitudes of the input and transmitted waves. $\gamma' = 0$ for the local grating, while $\gamma'' = 0$ for the nonlocal grating. The nonlocal grating gives rise to the unidirectional energy transfer from one beam to another. The gain factor for intensities is used commonly for characterization of this energy transfer. The intensity of the transmitted signal is described with it as $I_S = I_S^0 \exp(\Gamma d)$ in the undepleted pump approximation, where d is the interaction length.

The spectrum of the TWM signal may be obtained for the nondegenerate frequency interaction when the frequency detuning Ω is introduced in one of the recording waves. For a photorefractive grating the spectrum of the coupling constant has a Lorentzian shape[11]

$$\Gamma = \Gamma_0 \Big/ \left(1 + \Omega^2 \tau_{SC}^2\right), \tag{4}$$

where $\Gamma_0 = 2\gamma'$ is the maximum gain factor, which is observed at $\Omega = 0$, and τ_{SC} is the grating response time. The local grating does not enable energy transfer in the steady state, as the nonlocal grating does. However, the energy transfer may appear when frequency detuning is introduced: The nonlocal component of the grating occurs when the running hologram follows the interference pattern with a delay defined by the response time. This nonlocal component enables energy transfer. Therefore, the spectrum of the gain factor can be considered for the local gratings, too. It has the dispersion-like shape

$$\Gamma = \Gamma_0 \; \Omega \tau_{SC} \Big/ \left(1 + \Omega^2 \tau_{SC}^2\right), \tag{5}$$

where $\Gamma_0 = 2|\gamma''|$ now.

The TWM gain spectra for the nonlocal and local gratings calculated from Eqs. (4,5) are presented in Fig. 2a,b, respectively, in dimensionless coordinates $\Gamma/\Gamma_0 = f(\Omega \tau_{SC})$. They have very different shapes. That is why we use in what follows the shapes of the gain spectra measured at different experimental conditions as indicators of the type of response.

4. EXPERIMENTAL RESULTS AND DISCUSSION

The studied CdTe:Ge crystal was grown in Chernivtsy National University, Ukraine. The input faces parallel to (110) plane are optically polished while silver-paste electrodes are deposited on the side faces parallel to (111) plane. An external dc voltage is applied to the electrodes, forming an electric field E_0 along the [111] axis. The interaction length of the rectangular sample $d = 0.7$ cm, while the interelectrode distance $l = 0.4$ cm.

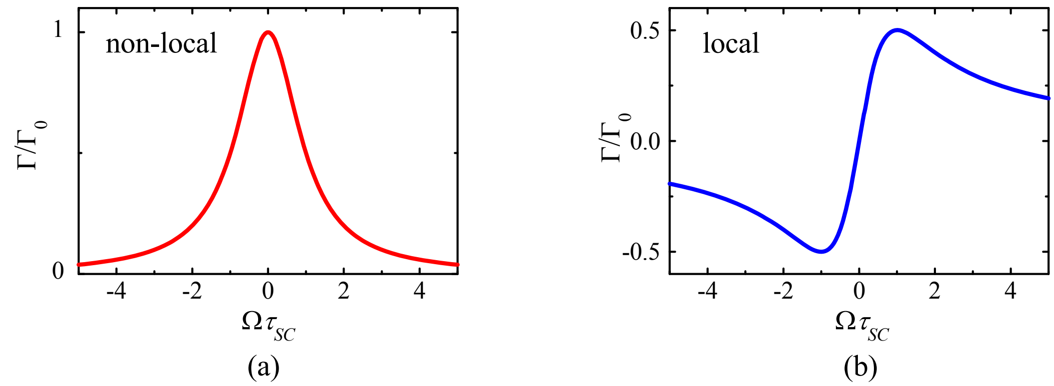

Figure 2. Spectral profiles of the gain factor in TWM with (a) – nonlocal and (b) – local response.

The experimental setup is shown in Fig. 3. A single-frequency cw laser operating at λ = 1064 nm with a total output power P = 500 mW serves as the light source. The output laser beam is divided by a beam splitter into two beams I_S^0 and I_P^0 with intensity ratio $\beta \approx$ 1:10. Both beams are expanded to ensure homogeneous illumination over the crystal cross-section. The total light intensity on the crystal input face is I = 30 mW/cm^2. The beams polarized in the plane of incidence enter the sample through the (110) face and record a grating with grating vector parallel to [111] axis. Such a recording geometry ensures the largest effective electro-optic coefficient for transmission gratings in the cubic CdTe crystal[12]. A calibrated electro-optic modulator EOM introduces frequency detuning Ω into the weak signal wave. The intensity of the signal is measured with and without the pump beam for evaluation of the gain factor.

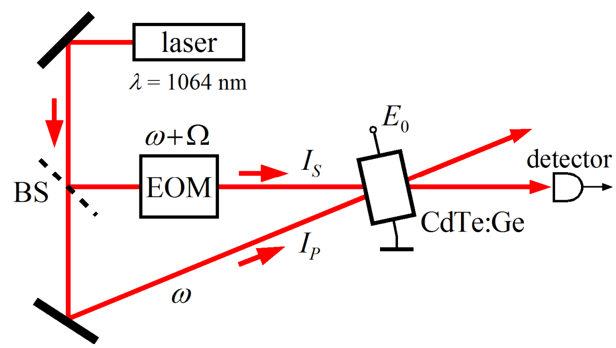

Figure 3. Experimental setup; BS – beam-splitter, EOM – electro-optic modulator.

The spectrum of the gain factor measured without electric field at a grating spacing Λ = 1 μm is shown by squares in Fig. 4a. The profile is symmetrical with maximum gain at zero frequency detuning, as is expected for the local grating. However, the shape of the spectrum is narrower than the Lorenzian one expected from Eq. (4). Such narrowing can be explained by the intensity change along the propagation path due to absorption[13]. The time constant changes also in the crystal and an overall response becomes more complicated. The complex space charge formation in CdTe:Ge[14] with different time constants for participating processes[15] is probably important, too.

To test the ability of the set-up for ultrasound detection the EOM is set to introduces a fast small phase modulation $\varphi(t) = \Delta\varphi \sin(2\pi f t)$ with $\Delta\varphi$ = 0.15 rad and f = 50 kHz ($2\pi f t >> 1/\tau_{SC}$) instead of the frequency detuning Ω. A small intensity modulation with SNR < 1 is observed at the doubled frequency $2f$, as is expected from Eq. (3) for a nonlocal grating. The amplitude of the intensity modulation $\Delta I_S/I_S^{mean}$ < 0.5%. So, the type of response should be changed and this change should manifest itself in the shape of the spectrum. The photorefractive gratings give many different possibilities for the change of the spectral response. For example, two gratings formed by waves with different frequency detunings may form a two-maxima gain profile, which can be used for gravitational waves detection[16]. We use an electric field to change the type of response.

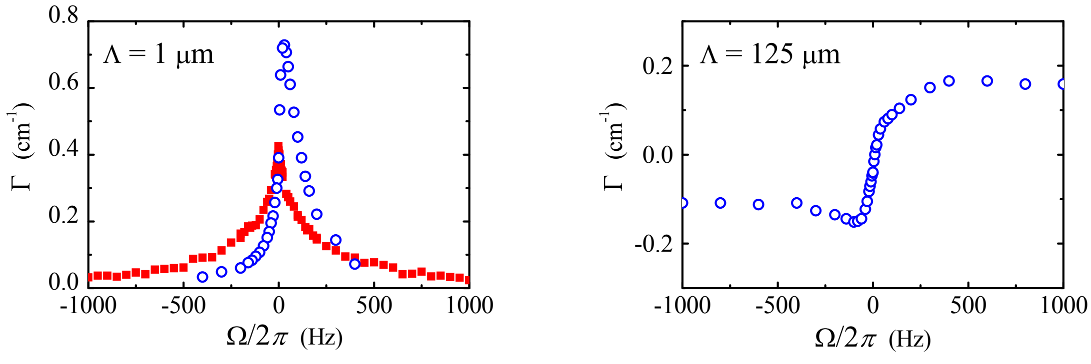

Figure 4. Spectral profiles of the gain factor in TWM measured at (a) – $\Lambda = 1$ μm with no field (squares) and with dc field $E_0 = 4$ kV/cm (circles); (b) – at $\Lambda = 125$ μm with dc field $E_0 = 4$ kV/cm.

The spectrum measured with a dc field $E_0 = 4$ kV/cm at the same grating spacing $\Lambda = 1$ μm is shown by circles in Fig. 4a. The spectrum is changed under a dc field and the maximum gain factor increases nearly two times, but the shape of the spectrum remains closer to the Lorenzian than to the dispersion-like profile. This is because the nonlocal component of the grating still dominates. Such behavior is expected until the drift length becomes much smaller than the grating spacing[17]. At the same time the local component of the grating is quite significant even at this grating spacing. It is confirmed by a much larger intensity modulation $\Delta I_S/I_S^{mean} \approx 6.5\%$, which is now at the same frequency f as the input phase modulation.

A stronger local component of the grating is observed in the presence of a dc field at larger grating spacing, as is expected[17]. Experimental results measured at $\Lambda = 125$ μm are shown in Fig. 4b. The spectrum has almost dispersion-like profile, which confirms the recording of the local grating.

The narrow resonances in the vicinity of zero frequency detuning shown in Fig. 4a and the corresponding nonlinear dispersion are important for some spectacular phenomena like light pulse slowing down with photorefractive wave mixing[18,19]. The phase-to-intensity conversion is performed outside of these resonances at larger frequencies, where the index grating may be considered as a fixed grating. In other words, the phase-to-intensity conversion is a linear process. The nonlinear response of the dynamic grating with its response time is important for the adaptive capability of the TWM interferometer. The interferometer works as a high-pass filter, compensating for low frequency disturbances. To demonstrate the temporal adaptability of the grating in CdTe:Ge, the frequency response of the adaptive interferometer is studied. The normalized amplitude of the intensity modulation measured as a function of phase modulation frequency for a fixed phase modulation amplitude $\Delta\varphi = 0.15$ rad is shown in Fig. 5 by squares.

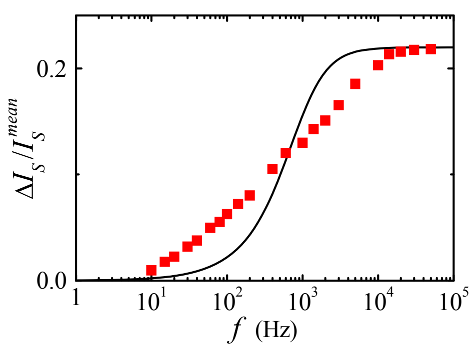

Figure 5. Normalized amplitude of intensity modulation as a function of phase modulation frequency measured at $\Lambda = 125$ μm with a dc field $E_0 = 4$ kV/cm.

The frequency response is characterized usually by the cutoff frequency measured at half-level of the maximum modulation amplitude. The cutoff frequency $f_C \approx 600$ Hz is estimated from the data of Fig. 5. The theory predicts that

$$\Delta I_S = \Delta I_S^{sat} \frac{2\pi f \tau_{SC}}{\sqrt{1+\left(2\pi f \tau_{SC}\right)^2}}, \tag{6}$$

where ΔI_S^{sat} is the intensity modulation in saturation at high frequency. The solid line in Fig. 5 represents the best fit of Eq. (6) to the experimental data with τ_{SC} = 160 μs and a maximum modulation amplitude $\Delta I_S^{sat}/I_S^{mean} \approx 0.22$. The discrepancy between the experimental data and the theory may be explained again by the complicated space charge formation in CdTe:Ge and by the response time variation inside the crystal because of the linear absorption. The increased response of the interferometer at low frequency often is undesirable, but it may be suppressed considerably by temperature control of the crystal slightly above the room temperature[20].

The maximum modulation amplitude at high frequency characterizes the sensitivity of an adaptive interferometer for measurement of small displacements. It can be used for comparison of different systems. The relative detection limit δ_{rel} was introduced as the ratio of sensitivity of an adaptive interferometer to that of a classical plane-wave interferometer. For a local dynamic grating it can be found experimentally[21]

$$\delta_{rel} = \frac{\exp\left(\alpha d/2\right)}{\left|\sin\left(\gamma'' d\right)\right|}. \tag{7}$$

Using the correspondence between input phase modulation and output intensity modulation[10] $\Delta I_S^{sat}/I_S^{mean} = 2\sin(\gamma'' d)\Delta\varphi$ and absorption constant $\alpha \approx 1.2$ cm^{-1}, $\delta_{rel} \approx 2.1$ is estimated. This value is among the best values ever reported for adaptive interferometers operating at $\lambda = 1064$ nm.

5. CONCLUSIONS

Dramatic difference in the profiles of the amplification spectra in TWM on the local and nonlocal dynamic holograms can be used for identification of the type of response. The study of the TWM gain spectra in CdTe:Ge at different experimental conditions shows that an almost local response can be achieved in a dc-biased crystal at quite large grating spacing $\Lambda > 100$ μm because of the long drift length of the photoexcited charge carriers.

The operation of an adaptive interferometer with photorefractive a CdTe:Ge crystal is compared for (1) a nonlocal response in the diffusion mode of grating recording and (2) a local response initiated by an external dc field. Fundamental improvement of the performance of TWM interferometer is demonstrated, when changing the dynamic hologram from a nonlocal to a local one. Excellent characteristics of the interferometer are demonstrated. The relative detection limit $\delta_{rel} \approx 2.1$, which is the best according to our knowledge for TWM interferometers operating at $\lambda = 1064$ nm, is accompanied by high cutoff frequency $f_C \approx 600$ Hz at a low intensity $I = 30$ mW/cm^2. The better detection limit is expected for a larger dc field, while the cutoff frequency may be increased with intensity increase.

6. ACKNOWLEDGEMENTS

Partial financial support of the European Office of Aerospace Research & Development (grant 118006) through the Science and Technology Center in Ukraine (Project P585a) is gratefully acknowledged. The authors thank Z. I. Zakharuk for the CdTe:Ge crystal.

REFERENCES

[1] Davidson, F. M. and Boutsikaris, L., "Homodyne detection using photorefractive materials as beamsplitters," Opt. Eng. 29(4), 369-377 (1990).

[2] Rossomakhin I. M. and Stepanov, S. I., "Linear adaptive interferometers via diffusion recording in cubic photorefractive crystals," Opt. Commun. 86(2), 199-204 (1991).
[3] Ing, R. K. and Monchalin, J. P., "Broadband optical detection of ultrasound by two-wave mixing in a photorefractive crystal," Appl. Phys. Lett. 59(25), 3233-3235 (1991).
[4] Di Girolamo, S., Kamshilin, A. A., Romashko, R. V., Kulchin, Yu. N. and Launay, J. C., "Fast adaptive interferometer on dynamic reflection hologram in CdTe:V," Opt. Express 15(2), 545-555 (2007).
[5] Shcherbin, K. and Klein, M. B. "Adaptive interferometers with no external field using reflection gratings in CdTe:Ge at 1550 nm," Optics Commun. 282(13), 2580-2585 (2009).
[6] Bortolozzo, U., Residori, S. and Huignard, J. P., "Adaptive holography in liquid crystal light-valves," Materials 5(9), 1546-1559 (2012).
[7] Jayet, B., Huignard, J. P. and Ramaz, F., "Refractive index and gain grating in Nd:YVO_4: application to speckle vibrometry and photoacoustic detection," Opt. Lett. 42(4), 695-698 (2017).
[8] Bortolozzo, U., Dolfi, D., Huignard, J. P., Molin, S., Peigné, A. and Residori, S., "Self-adaptive vibrometry with CMOS-LCOS digital holography," Opt. Lett. 40(7), 1302-1305 (2015).
[9] Staebler, D. L. and Amodei, J. J., "Coupled-wave analysis of holographic storage in $LiNbO_3$," J. Appl. Phys. 43(3), 1042-1049 (1972).
[10] Delaye, Ph., Blouin, A., Drolet, D., de Montmorillon, L. A., Roosen, G. and Monchalin, J. P., "Detection of ultrasonic motion of a scattering surface by photorefractive InP:Fe under an applied dc field," J. Opt. Soc. Am. B 14(7), 1723-1734 (1997).
[11] Yeh, P., [Introduction to Photorefractive Nonlinear Optics] Wiley, New York (1993).
[12] Odoulov, S. G., Slussarenko, S. S. and Shcherbin, K. V. "Energy exchange during the recording of dynamic displacement gratings in cadmium telluride," Sov. Tech. Phys. Lett. 15(2) 417-418 (1989).
[13] Brost, G., Norman, J., Odoulov, S., Shcherbin, K., Shumelyuk, A. and Taranov, V., "Gain spectra of beam coupling in photorefractive semiconductor," J. Opt. Soc. Am. B 15(7), 2083-2091 (1998).
[14] Briat, B., Shcherbin, K., Farid, B. and Ramaz, F., "Optical and magnetooptical study of photorefractive germanium-doped cadmium telluride," Opt. Commun. 156(4-6), 337-340 (1998).
[15] dos Santos, T. O., Frejlich, J. and Shcherbin, K., "Photo electromotive force in CdTe:Ge: manifestation of two photorefractive centers," Appl. Phys. B 99(4), 701-707 (2010).
[16] Yum, H. N., Salit, M., Pati, G. S., Tseng, S., Hemmer, P. R. and Shahriar, M. S., "Fast-light in a photorefractive crystal for gravitational wave detection," Opt. Express 16(25), 20448-20456 (2008).
[17] Kukhtarev, N. V., Markov, V. B., Odulov, S. G. Soskin, M. S. and Vinetskii, V. L., "Holographic storage in electrooptic crystals. I. Steady state," Ferroelectrics 22(1), 949-960 (1978).
[18] Podivilov, E., Sturman, B., Shumelyuk, A. and Odoulov, S., "Light pulse slowing down up to 0.025 cm/s by photorefractive two-wave coupling," Phys. Rev. Lett. 91(8), 083902 (2003).
[19] Mathey, P., Gadret, G. and Shcherbin, K., "Slow light with degenerate backward-wave four-wave mixing," Appl. Phys. B 102(3), 539-543 (2011).
[20] Shcherbin, K., Danylyuk, V. and Klein, M. B., "Characteristics of two-wave mixing adaptive interferometer with CdTe:Ge at 1.06 and 1.55 μm and improved temporal adaptability with temperature control," App. Opt. 52(12) 2729-2734 (2013).
[21] de Montmorillon, L. A., Delaye, Ph., Launay, J. C. and Roosen, G., "Novel theoretical aspects on photorefractive ultrasonic detection and implementation of a sensor with an optimum sensitivity," J. Appl. Phys. 82(12), 5913-5922 (1997).